JOURNAL OF GUIDANCE, CONTROL, AND DYNAMICS
Vol. 26, No. 5, September–October 2003

Statistical Analysis of Control Maneuvers in Unstable Orbital Environments

C. A. Renault* and D. J. Scheeres†
University of Michigan, Ann Arbor, Michigan 48109-2140

The optimal placement of statistical control maneuvers is analyzed for maintaining position near an unstable equilibrium point. This idea is developed for the libration points in the Hill three-body problem, but the analysis can be generalized to other unstable systems and is applied to the restricted three-body problem as well. First the basics of statistical fuel usage in the context of orbit determination errors and their mapping in time are reviewed. With use of linear theory, several explicit targeting formulas are devived for driving a spacecraft back to a fixed point. The mean and standard deviation of these schemes are analyzed for our special case, and explicit solutions for them are found. With use of these results the fuel-optimal spacing of the maneuvers in time can be devived to control a spacecraft to the vicinity of an unstable libration point. It is found that the optimal spacing is related to the characteristic time of the instability. It is also found that a linear quadratic regulator LQR control scheme will outperform control schemes that target the stable manifold of the equilibrium point.

Introduction

TO plan for the navigation of a spacecraft, it is necessary to develop a statistical model for the amount of fuel that will be needed to keep the spacecraft on course. In its most general form, the problem can be stated as follows. Given an error in position and velocity relative to the nominal trajectory at time t_0 of the form $\delta \boldsymbol{r}_0$, and $\delta \boldsymbol{v}_0$, what is the mean and variance in the cost of the maneuvers to reduce the system back to $\delta \boldsymbol{r} = \delta \boldsymbol{v} = 0$ at some future time? Generally, the errors in position and velocity arise from the previous maneuver and can be thought of as errors in knowledge of the spacecraft state. Practically, maneuver execution errors must also be incorporated, but we ignore these in this paper.

In this paper, we study this problem applied to motion near a hyperbolic unstable equilibrium point of a Hamiltonian system. For practical application, we discuss the case of the libration points in the Hill three-body problem and the L_1 and L_2 equilibrium points in the restricted three-body problem. For such time-invariant systems we find general analytical expressions for the mean and variance of the ΔV maneuvers necessary to maintain the spacecraft in the vicinity of the equilibrium point. These formulas are parameterized by the assumed level of orbit determination uncertainty, the timing of maneuvers, and the specific control law used. For a hyperbolic unstable equilibrium point, we find that the optimal timing of maneuvers is fundamentally related to the characteristic time of the hyperbolic instability. This relationship holds even as we consider different approaches to the control of a spacecraft in this environment. We consider three main variations of trajectory control. The first approach specifically targets the spacecraft back to the equilibrium point with a sequence of two maneuvers. The second approach targets the spacecraft back to the stable manifold of the equilibrium point, which then will bring the spacecraft back to the equilibrium point under the natural dynamics of the system. The third approach applies a discrete linear quadratic controller to the problem, which keeps the distance of the spacecraft from the equilibrium point bounded, but does not specifically target the spacecraft back to the equilibrium point. Among these three approaches, we find that the linear quadratic controller can give the minimum overall cost, which is expected, because it has additional parameters that allow the fuel cost to be optimized. Assuming specific orbit determination tracking accuracies, we are able to predict statistical fuel usage for maintaining a spacecraft in the vicinity of the L_1 and L_2 unstable equilibrium points of the Earth–sun and moon–Earth systems for an extended period of time. For the Earth–sun system, we find an optimal maneuver spacing of approximately 23 days, whereas for the moon–Earth system, we find an optimal maneuver spacing on the order of 1.5–2 days. The statistical cost of maintaining a libration point orbiter in the Earth–sun system is so small that it will, in general, be overwhelmed by maneuver execution and modeling errors. The same is not true for the moon–Earth system, however, where the statistical cost of maintaining position near an equilibrium point is on the order of 3 m/s per month.

This problem was considered for the standard two-body problem by Battin.[1] Many papers have also applied control analysis to motion in unstable libration point orbits. Farquhar et al.[2] outline the actual maneuvers performed for the International Sun–Earth Explorer (ISEE-3) mission, Howell and Pernicka[3] and Howell and Gordon[4] study the general libration orbiter control problem using numerical methods, Jones and Bishop[5] study this problem for the terminal guidance and control of a halo orbiter, Cielaszyk and Wie[6] apply digital control techniques to this problem, Gomez et al.[7] apply dynamic systems theory to their consideration of halo orbit control, and Scheeres et al.[8] apply a low-thrust feedback control that stabilizes an unstable halo orbit. A review of halo orbit control techniques used in practice has been given by Dunham and Roberts.[9] In this paper, we reconsider the question of optimal timing of control maneuvers given statistical errors in orbit determination.[10] The analysis given here differs from these previous works in two ways. First, we consider the idealized problem of controlling a spacecraft in the vicinity of a libration point, as opposed to the vicinity of a halo orbit; later in this section we argue that the general results found for our system can be extended to more general unstable orbits. Second, we find closed-form solutions for the mean and variance of the control ΔV needed for a number of different control strategies. This allows us to predict explicitly the statistical fuel usage as an analytical function of orbit determination uncertainties, control strategy, and the timing of control maneuvers. Our approach results in a general ability to compare and contrast directly different strategies, a feature not present in previous analyses.

Note that the analysis outlined in this paper concentrates on the statistical prediction of fuel usage for a spacecraft and does not necessarily represent the actual control strategy that would be used in

Presented as Paper 2002-4725 at the Astrodynamics Specialist Conference; received 15 July 2002; revision received 15 April 2003; accepted for publication 16 April 2003.

*Graduate Student Research Assistant, Department of Aerospace Engineering.

†Associate Professor, Department of Aerospace Engineering. Senior Member AIAA.

a mission. Indeed, for the design of correction maneuvers during a mission, there are other important operations constraints that must be included. At the least, the mission operations team usually reoptimizes the entire trajectory when designing control maneuvers; applications of this process to unstable orbits in the vicinity of the Earth–sun libration points is discussed by Wilson et al.[11] and Serban et al.[12] The practical application of the analysis performed in this paper applies to the premission phase, where predictions of fuel usage are being developed. For future missions, our analysis also points toward the automation of trajectory control maneuvers because we investigate the optimal use of very simple control algorithms for maintaining position about an unstable equilibrium.

Statistical Maneuver Design

For a general trajectory, a minimum of two maneuvers is required to get back on track: one maneuver to target back to the trajectory at some future time and a second maneuver to reduce the relative velocity to zero at that crossing. Of course, at the time when the trajectory crossing occurs, errors from the epoch of the last maneuver manifest themselves in a new set of dispersions, which must themselves be corrected. By considering the new dispersions to be uncorrelated with the initial dispersions (a conservative assumption in general), we can isolate these effects from each other and perform an analysis on the two maneuvers alone. For the design of these maneuvers, we have two free parameters, the time at which we perform the first correction maneuver, t_1, and the time at which the trajectory crossing (and the second maneuver) will occur, t_2. For a more general approach, we also derive a discrete linear quadratic controller and apply it to our problem, where now the control sequence consists of a maneuver of the same form after a characteristic time interval.

The cost of a general correction maneuver can always be expressed as a formula of the form

$$\Delta V_i = |\Psi_i \boldsymbol{x}_0| \tag{1}$$

where Ψ_i is a time-varying matrix in general and $\boldsymbol{x}_0$ is the state deviation measured at some initial epoch t_0. To compute the statistical cost of these maneuvers requires us to compute the mean and variance

$$\overline{\Delta V} = \int_\infty \Delta V f(\boldsymbol{x}_0)\,\mathrm{d}\boldsymbol{x}_0 \tag{2}$$

$$\sigma^2_{\Delta V} = \int_\infty (\Delta V - \overline{\Delta V})^2 f(\boldsymbol{x}_0)\,d\boldsymbol{x}_0 \tag{3}$$

$$= \overline{(\Delta V)^2} - \overline{\Delta V}^2 \tag{4}$$

Assume that the measurement noise has zero mean and a Gaussian distribution; the probability density function of the initial conditions can be written as

$$f(\boldsymbol{x}_0) = \frac{\sqrt{|\Lambda_0|}}{(2\pi)^{N/2}} \exp\left(-\tfrac{1}{2}\boldsymbol{x}_0^T \Lambda_0 \boldsymbol{x}_0\right) \tag{5}$$

where N is the total dimension of the system phase space and Λ_0 is the initial information matrix. In the Appendix specific formula are derived for the mean and variance computation of ΔV.

If we implement a series of M such maneuvers, each with the same assumed statistical and dynamic representation, the total mean maneuver cost is $M\overline{\Delta V}$ and the total variance is $M\sigma^2_{\Delta V}$. Thus, if we wish to estimate the statistical cost of performing this sequence of maneuvers to within an n-sigma probability value (one-dimensional Gaussian), we find

$$\Delta V_{\text{stat}} = M\left[\overline{\Delta V} + \left(n/\sqrt{M}\right)\sigma_{\Delta V}\right] \tag{6}$$

Thus, as the number of maneuvers becomes large, we see that the total (predicted) statistical cost can be approximated as

$$\Delta V_{\text{stat}} \sim M\overline{\Delta V} \tag{7}$$

Assume that we wish to control a trajectory over an extended period of time T_∞ and that we perform a maneuver (or repeat a maneuver sequence) after every time T, resulting in a total of $M = T_\infty / T$ maneuvers. Then the total statistical cost of this sequence of maneuvers is

$$\Delta V_{\text{stat}} \sim T_\infty(\overline{\Delta V}/T) \tag{8}$$

and for an arbitrary length of time T_∞, we see that to optimize fuel usage we need to choose the time interval between maneuvers T to minimize $\overline{\Delta V}/T$. In the following discussion, we will use a set definition for T equal to the time between the determination of the state error $\boldsymbol{x}_0$, t_0, and the first maneuver of our sequence, t_1.

Hill Model and Motion About the Libration Points

Scaling of the Equations

Let us introduce the three-dimensional equations for the Hill three-body problem (see Ref. 13),

$$\ddot{x} - 2\omega\dot{y} = -(\mu/r^3)x + 3\omega^2 x \tag{9}$$

$$\ddot{y} + 2\omega\dot{x} = -(\mu/r^3)y \tag{10}$$

$$\ddot{z} = -(\mu/r^3)z - \omega^2 z \tag{11}$$

where ω is the rotation rate of the secondary around the primary, $\mu = GM$, M is the mass of the secondary, and x, y, and z denote the position of the spacecraft in the vicinity of the secondary. Transforming these equations into nondimensional form gives us the length scale, $l = (\mu/\omega^2)^{1/3}$ and the timescale $1/\omega$. (For the restricted three-body problem, the length scale is instead the distance between the two primaries.) Let Λ_0 be the information matrix corresponding to these nondimensional equations, then

$$\Lambda_0 = \begin{bmatrix} 1/\sigma_r^2 & 0 \\ 0 & 1/\sigma_v^2 \end{bmatrix} \tag{12}$$

with $\sigma_r = \sigma_{rd}/l$ and $\sigma_v = \sigma_{vd}/(l\omega)$, and σ_{rd} and σ_{vd} correspond to the variance of the error in position and velocity, respectively, due to orbit determination errors. In the following, we will take $\sigma_{rd}/\sigma_{vd} = 10^6$. All of the following computations have been made using a nondimensional information matrix $\Lambda = \sigma_r^2\Lambda_0$, where

$$\Lambda_0 = \begin{bmatrix} 1 & 0 \\ 0 & \omega_E^2(\sigma_{rd}/\sigma_{vd})^2 \end{bmatrix} \tag{13}$$

The results of the nondimensional statistical analysis will be the mean maneuver cost rate with units of length over time squared, represented as $\Delta v/\Delta\tau$, where Δv is the mean maneuver cost and $\Delta\tau$ is the time interval between maneuvers. Even though the normalized Hill problem has no parameter, there is a parameter in the information matrix, $\omega^2(\sigma_{rd}/\sigma_{vd})^2$, which varies according to the ratio of position to velocity accuracy and with the rotation rate of the secondary about the primary. An additional parameter is $\sigma_r = \sigma_{rd}/l$. Unless otherwise specified, the value $\Delta v/\Delta\tau$ will be shown. To transform these to dimensional costs in kilometers per second squared, we use

$$\Delta v_d/\Delta t = \sigma_{rd}\omega^2(\Delta v/\Delta\tau) \tag{14}$$

To get the maneuver rate in kilometers per second per secondary period

$$\Delta v_d/\Delta t = 2\pi\sigma_{rd}\omega(\Delta v/\Delta\tau) \tag{15}$$

Libration Points of the Hill Problem

The general nondimensional equations of motion for the Hill three-body problem are found from Eqs. (9–11) by setting $\mu = \omega = 1$. This system has two equilibrium points, $x = \pm 3^{-1/3}$ and $y = z = 0$. As the linear motion along the z axis is decoupled from linearized motion in the x–y plane, the following analysis will consider motion only in the x–y plane. Let us linearize the system around the equilibrium points $x = \pm 3^{-1/3}$, using $\delta \boldsymbol{x} = [\delta x \quad \delta y \quad \delta \dot{x} \quad \delta \dot{y}]^T$,

$$\delta \dot{\boldsymbol{x}} = \begin{bmatrix} 0 & 0 & 1 & 0 \\ 0 & 0 & 0 & 1 \\ 9 & 0 & 0 & 2 \\ 0 & -3 & -2 & 0 \end{bmatrix} \delta \boldsymbol{x} \tag{16}$$

Let us call the preceding matrix U. Integrating this equation gives $\delta \boldsymbol{x} = \Phi(t, t_0, \boldsymbol{x}_0)\delta \boldsymbol{x}_0$ with

$$\Phi(t, t_0, \boldsymbol{x}_0) = e^{U(t - t_0)} \tag{17}$$

The eigenvalues of U are $\pm\lambda_1 = \pm\sqrt{[1 + 2\sqrt{(7)}]}$ and $\pm j\lambda_2 = \pm j\sqrt{[2\sqrt{(7)} - 1]}$. The eigenvectors corresponding to these eigenvalues define the direction of the stable and unstable manifolds in phase space. Writing $e^{Ut} = \alpha_1 U^3 + \alpha_2 U^2 + \alpha_3 U + \alpha_4 I$, for each eigenvalue λ we find

$$e^{\lambda t} = \alpha_1\lambda^3 + \alpha_2\lambda^2 + \alpha_3\lambda + \alpha_4 \tag{18}$$

Solving this system leads to

$$\alpha_1 = \frac{\sinh(\lambda_1 t)/\lambda_1 - \sinh(\lambda_2 t)/\lambda_2}{\lambda_1^2 + \lambda_2^2} \tag{19}$$

$$\alpha_2 = \frac{\cosh(\lambda_1 t) - \cosh(\lambda_2 t)}{\lambda_1^2 + \lambda_2^2} \tag{20}$$

$$\alpha_3 = \frac{\lambda_2^2 \sinh(\lambda_1 t)/\lambda_1 + \lambda_1^2 \sinh(\lambda_2 t)/\lambda_2}{\lambda_1^2 + \lambda_2^2} \tag{21}$$

$$\alpha_4 = \frac{\lambda_2^2 \cosh(\lambda_1 t) + \lambda_1^2 \cosh(\lambda_2 t)}{\lambda_1^2 + \lambda_2^2} \tag{22}$$

Computing U^2 and U^3 and replacing the α_i by their values gives $\Phi(t, t_0, \boldsymbol{x}_0) = [\Phi_1 \quad \Phi_2]$,

$$\Phi_1 = \frac{1}{2\sqrt{7}} \begin{bmatrix} \sqrt{7}a + 4b & -3c \\ -9c & \sqrt{7}a - 2b \\ 9(2c + \sqrt{7}d) & -3b \\ -9b & 3(4c - \sqrt{7}d) \end{bmatrix} \tag{23}$$

$$\Phi_2 = \frac{1}{2\sqrt{7}} \begin{bmatrix} 2c + \sqrt{7}d & b \\ -b & -(4c - \sqrt{7}d) \\ \sqrt{7}a + 2b & c + 2\sqrt{7}d \\ -(c + 2\sqrt{7}d) & \sqrt{7}a - 4b \end{bmatrix} \tag{24}$$

where

$$a = \cosh(\lambda_1 t) + \cos(\lambda_2 t), \qquad b = \cosh(\lambda_1 t) - \cos(\lambda_2 t)$$

$$c = [\sinh(\lambda_1 t)/\lambda_1] - [\sin(\lambda_2 t)/\lambda_2]$$

$$d = [\sinh(\lambda_1 t)/\lambda_1] + [\sin(\lambda_2 t)/\lambda_2]$$

Because this gives us the general expression of $\Phi(t, t_0, \boldsymbol{x}_0)$, the computation of the matrix exponential is not needed.

Control Strategies

Two-Maneuver Control Sequence

In this section, the statistical cost of two maneuvers performed at different times is computed. A maneuver ΔV_1 is made at $t_1 = n\Delta\tau$ based on a solution at time t_0 to null the error in position at time t_2, and a maneuver ΔV_2 is made at $t_2 = n\Delta\tau + (t_2 - t_1)$ to null the error in velocity. Let

$$\Phi = \begin{bmatrix} \phi_{rr} & \phi_{rv} \\ \phi_{vr} & \phi_{vv} \end{bmatrix} \tag{25}$$

$$\phi_1(t_2, t_1) = \phi_{rv}^{-1}(t_2, t_1)\phi_{rr}(t_2, t_1) \tag{26}$$

$$\phi_2(t_2, t_1) = \phi_{vv}(t_2, t_1)\phi_{rv}^{-1}(t_2, t_1)\phi_{rr}(t_2, t_1) - \phi_{vr}(t_2, t_1) \tag{27}$$

Then

$$\Delta V_1 = -[\phi_1(t_2, t_1)\phi_{rr}(t_1, t_0) + \phi_{vr}(t_1, t_0)]\delta \boldsymbol{r}_0$$

$$-[\phi_1(t_2, t_1)\phi_{rv}(t_1, t_0) + \phi_{vv}(t_1, t_0)]\delta \boldsymbol{v}_0 \tag{28}$$

$$\Delta V_2 = \phi_2(t_2, t_1)[\phi_{rr}(t_1, t_0)\delta \boldsymbol{r}_0 + \phi_{rv}(t_1, t_0)\delta \boldsymbol{v}_0] \tag{29}$$

When the notation of the Appendix is used, the computation of $\overline{|\Delta V|}$ is made using $K = \Lambda$ and for $\overline{|\Delta V_1|}$, $\Psi = \Psi_1$ ($\Delta V_1 = \Psi_1 \delta \boldsymbol{x}_0$), and for $\overline{|\Delta V_2|}$, $\Psi = \Psi_2$ ($\Delta V_2 = \Psi_2 \delta \boldsymbol{x}_0$). The general formula is

$$\overline{\Delta V} = \sqrt{2/\pi}\sqrt{\lambda + \mu} \quad \text{elliptic}E\left[\sqrt{2\mu/(\lambda + \mu)}\right] \tag{30}$$

with

$$\lambda = \left(a_1^T K^{-1} a_1 + \overline{a_2}^T K^{-1} \overline{a_2}\right)/2 \tag{31}$$

$$\mu = \sqrt{\left(a_1^T K^{-1} a_1 - \overline{a_2}^T K^{-1} \overline{a_2}\right)^2/4 + \left(a_1^T K^{-1} \overline{a_2}\right)^2} \tag{32}$$

$$\Psi = \begin{bmatrix} a_1 \\ \overline{a_2} \end{bmatrix} \tag{33}$$

where elliptic$E$ is the complete elliptic integral of the second kind. Figure 1 shows the variation of the minimum of the costs when the interval $t_2 - t_1$ is varying. For each value of $t_2 - t_1$, the total cost $(\overline{|\Delta V_1|} + \overline{|\Delta V_2|})/(t_1 - t_0)$ is computed for a range of values of $t_1 - t_0$ to find the minimum cost. Figure 1 shows that the influence of this period is important only when $t_2 - t_1$ is such that the matrix ϕ_{rv} is singular. At $t_2 - t_1$ constant, the minimum occurs for $\Delta\tau = 0.4$, quite close to the characteristic time of the unstable mode, $1/\lambda_1$. Then, the minimum of the cost varying $t_2 - t_1$ is the same in each interval, about 46.2. The cost has been computed taking the nondimensional

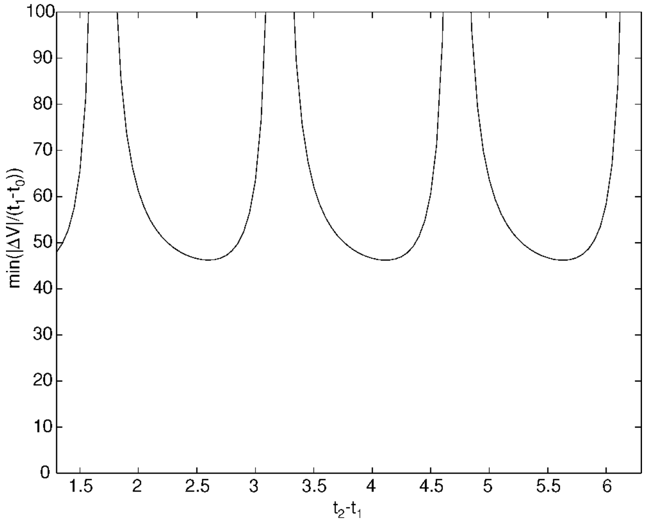

Fig. 1 Separated maneuvers: optimal cost varying $t_2 - t_1$.

norm of the velocity needed to correct the position divided by the nondimensional period between the maneuvers $\Delta\tau$.

Overlaid Two-Maneuver Control Sequences

The maneuvers to null the position at $t_2 + \Delta\tau$ and to null the velocity at t_2 can be performed simultaneously. Because only the magnitude of the velocity is important for computing the optimal cost, we hope to find a better minimum for $|\Delta V_1 + \Delta V_2|$ than for $|\Delta V_1| + |\Delta V_2|$. More generally, the case $t_2 - t_1 = k(t_1 - t_0)$, where k is an integer, will also be investigated.

Correction in Computation of the Mean and the Variance

At time $t_2 = n\tau$, two maneuvers are performed simultaneously: one maneuver to null the position at a time τ later and one to null the velocity due to the previous correction. The new correction is $\Delta V = \Delta V_1 + \Delta V_2$, where $\Delta V_1 = \Psi_1 \delta\boldsymbol{x}_1$ is the correction to null the state error $\delta\boldsymbol{x}_1$ determined τ before and $\Delta V_2 = \Psi_2 \delta\boldsymbol{x}_0$ is the correction to null the velocity due to the error $\delta\boldsymbol{x}_0$ determined 2τ before. Therefore, the new correction ΔV depends on two independent Gaussian variables $\delta\boldsymbol{x}_1$ and $\delta\boldsymbol{x}_0$.

When the notation of the Appendix is used, the computation is made using Eq. (30): $\Psi = [\Psi_1 \Psi_2]$ 8×2 and matrix

$$K = \begin{bmatrix} \Lambda & 0 \\ 0 & \Lambda \end{bmatrix}$$

Note that we have the freedom to introduce different error statistics for $\delta\boldsymbol{x}_0$ and $\delta\boldsymbol{x}_1$, but we keep them equal for simplicity.

Optimization of $\overline{|\Delta V|} = \overline{|\Delta V_1 + \Delta V_2|}$ *When* $t_2 - t_1 = k(t_1 - t_0)$

Let us now plot the cost of the maneuvers when the maneuver to null the position and the maneuver to null the velocity are made at the same time. Figure 2 shows the curves corresponding to the cost of the simultaneous maneuvers, the cost of the maneuver to null the position alone, ΔV_1, the cost to null the velocity alone, ΔV_2, and the sum of these two maneuvers if they were done separately. As expected, the cost of the maneuvers done separately is higher than the cost of the maneuvers done simultaneously. A minimum of 53.3 is achieved when the maneuvers are made separately and $t_2 - t_1 = t_1 - t_0 = 0.54$. (This is worse than the minimum obtained by varying $t_2 - t_1$.) When the maneuvers are made simultaneously, the new optimal time interval is $T = 0.54$ and the new minimum is 45.1, reducing the cost of the maneuvers by 2.4%. Let us now compare the values of the period and of the minimum when $t_2 - t_1 = k(t_1 - t_0)$. In this case, maneuvers are made every time interval τ, targeting the equilibrium point a time $k\tau$ later. Figure 3 shows that a new problem arises when k varies. When $t_2 - t_1$ is such that ϕ_{rv} is singular, the linear corrections become infinite. For $k = 3$, the new optimal cost is 37.5 for a period $T = 0.4$. Evaluating higher values of k gives other minimums around 38, none better than the preceding one. As a consequence, a new optimal cost is found for simultaneous maneuvers and $k = 3$. In comparison with the separated maneuvers, it improves the cost by 18.8%.

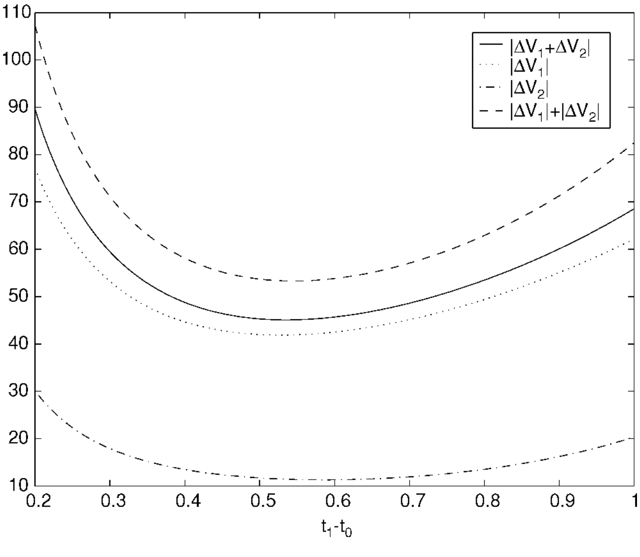

Fig. 2 Comparison of simultaneous, $t_2 - t_1 = t_1 - t_0$, and separated maneuvers: $k = 1$.

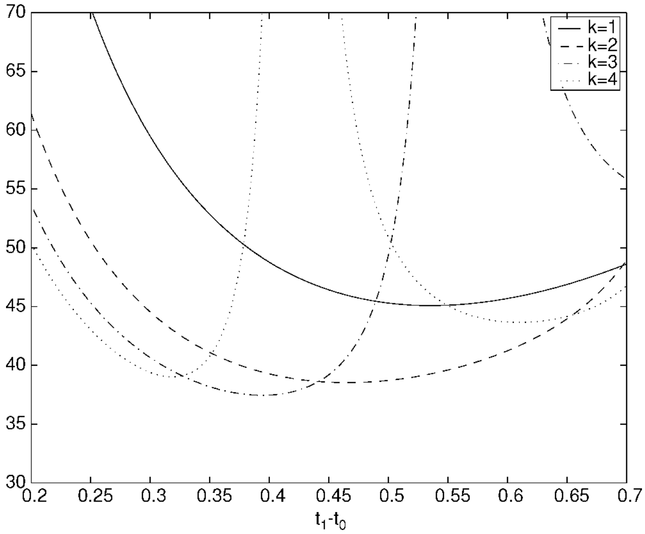

Fig. 3 Simultaneous maneuvers, $t_2 - t_1 = k(t_1 - t_0)$: optimal cost.

Stable Manifold Targeting

Computation of Optimal Cost When Targeting the Stable Manifold

Another approach to control is to make corrections to target the spacecraft to a state vector corresponding to the stable manifold of the equilibrium point. We hope to decrease the cost of the maneuvers by targeting a point in state space closer than the origin. Let us write the new ΔV_1 and ΔV_2 using $\boldsymbol{u}_s$ as the standard direction on which we want to target the spacecraft, where $[\boldsymbol{u}_s \;\; -\lambda_1 \boldsymbol{u}_s]$ is the eigenvector corresponding to the stable manifold. As a result, the final position of the spacecraft at t_2, after the second maneuver, will be $\eta[\boldsymbol{u}_s \;\; -\lambda_1 \boldsymbol{u}_s]$, and the spacecraft should approach the equilibrium point along the stable manifold. Then with $t = t_2 - t_1$, if $\delta\boldsymbol{r}_1$ and $\delta\boldsymbol{v}_1$ specify the position and velocity at the time t_1 of the first maneuver,

$$\Delta V_1 = \phi_{rv}(t)^{-1}[\eta_1 \boldsymbol{u}_s - \phi_{rr}(t)\delta\boldsymbol{r}_1] - \delta\boldsymbol{v}_1 \quad (34)$$

$$\Delta V_2 = \left(-\lambda_1 I - \phi_{vv}\phi_{rv}^{-1}\right)\eta_2 \boldsymbol{u}_s + \left(\phi_{vv}\phi_{rv}^{-1}\phi_{rr} - \phi_{vr}\right)\delta\boldsymbol{r}_1 \quad (35)$$

Let us minimize $|\Delta V_1|$, $\Delta V_1 = \eta_1 \boldsymbol{v}_s(t) + \phi_1 \boldsymbol{x}_1 = \eta_1 \boldsymbol{v}_s(t) + \boldsymbol{y}$, where $\boldsymbol{v}_s(t) = \phi_{rv}^{-1}\boldsymbol{u}_s$. The quantity $|\eta_1 \boldsymbol{v}_s(t) + \boldsymbol{y}|$ is minimized for $\eta_1 = -(\boldsymbol{y}^T \boldsymbol{v}_s / \boldsymbol{v}_s^T \boldsymbol{v}_s)$, which gives

$$|\Delta V| = \sqrt{\boldsymbol{y}^T\boldsymbol{y} - \frac{\left(\boldsymbol{y}^T \boldsymbol{v}_s\right)^2}{\boldsymbol{v}_s^T \boldsymbol{v}_s}} \quad (36)$$

With the notation of the Appendix and $\boldsymbol{v}_s = [v_{s1} \;\; v_{s2}]$,

$$|\Delta V_1| = \sqrt{(1 + \gamma^2)u_1^2 + u_2^2 + 2\gamma u_1 u_2 - C} \quad (37)$$

with

$$C = \frac{[u_1 v_{s1} + (u_2 + \gamma u_1)v_{s2}]^2}{v_{s1}^2 + v_{s2}^2} \quad (38)$$

Rearranging this expression gives

$$|\Delta V_1| = \frac{|(\gamma v_{s1} - v_{s2})u_1 + v_{s1} u_2|}{\sqrt{v_{s1}^2 + v_{s2}^2}} \quad (39)$$

Taking for the new variables $(v_1, v_2) = [\sqrt{(\alpha)}u_1; \sqrt{(\beta)}u_2]$ and then changing to polar coordinates gives the following new expression for the integral:

$$\overline{|\Delta V_1|} = \frac{1}{\sqrt{2\pi}} \times \int_0^{2\pi} \frac{\left|\left[(\gamma v_{s1} - v_{s2})\big/\sqrt{\alpha}\right]\cos\theta + \left(v_{s1}\big/\sqrt{\beta}\right)\sin\theta\right|}{\sqrt{v_{s1}^2 + v_{s2}^2}}\,\mathrm{d}\theta \tag{40}$$

Finally,

$$\overline{|\Delta V_1|} = \sqrt{\frac{2}{\pi}}\sqrt{\frac{m_{22}v_{s1}^2 + v_{s2}^2 - 2m_{12}v_{s1}v_{s2}}{v_{s1}^2 + v_{s2}^2}} \tag{41}$$

with $m_{11} = a_1^T\Lambda^{-1}a_1$, $m_{22} = \overline{a_2}^T\Lambda^{-1}\overline{a_2}$, and $m_{12} = a_1^T\Lambda^{-1}\overline{a_2}$. Equation (41) can be used only when $|\Delta V|$ is obtained minimizing $|\eta\boldsymbol{v}_s + \Psi\boldsymbol{x}|$. When $|\Delta V|$ takes the particular form $|\eta_1\boldsymbol{v}_s + \eta_2\boldsymbol{w}_s + \Psi\boldsymbol{x}|$, $\overline{|\Delta V|}$ can be obtained using the solution given by the Appendix for particular expression of η_1 and η_2 depending linearly on the $\delta\boldsymbol{r}_i$.

Computable Solutions

The first try made consists in minimizing only ΔV_1. As a result, the stable manifold is targeted such that $|\eta_1\boldsymbol{v}_s + \phi_1\delta\boldsymbol{r}_i|$ is minimized, that is,

$$\eta_i = -\frac{\boldsymbol{v}_s^T\phi_1\delta\boldsymbol{r}_i}{\boldsymbol{v}_s^T\boldsymbol{v}_s} \tag{42}$$

With use of the notation of the Appendix,

$$\Psi_1^{\text{new}} = \left(\frac{Id - \boldsymbol{v}_s\boldsymbol{v}_s^T}{\boldsymbol{v}_s^T\boldsymbol{v}_s}\right)\Psi_1 \tag{43}$$

$$\Psi_2^{\text{new}} = \Psi_2 - \frac{\boldsymbol{w}_s\boldsymbol{v}_s^T\phi_1}{\boldsymbol{v}_s^T\boldsymbol{v}_s} \tag{44}$$

What would seem a fortiori the best optimization here, minimizing $|\Delta V_1| + |\Delta V_2|$ is rather difficult to implement. Indeed, as will be shown in the following part, this minimization leads to resolving a polynomial of the fourth order and taking the root that gives the minimum. There is no algebraic solution to this problem, and η will not depend linearly on $\delta\boldsymbol{r}_i$. As a result, the integral will be difficult to compute. To simplify the problem, let us minimize $|\Delta V_1|^2 + |\Delta V_2|^2$ instead. This leads to

$$\eta_i = -\frac{\boldsymbol{v}_s^T\phi_1\delta\boldsymbol{r}_i + \boldsymbol{w}_s^T\phi_2\delta\boldsymbol{r}_i}{\boldsymbol{v}_s^T\boldsymbol{v}_s + \boldsymbol{w}_s^T\boldsymbol{w}_s} \tag{45}$$

with $\boldsymbol{w}_s = -(\lambda_1 I + \phi_{vv}\phi_{rv}^{-1})\boldsymbol{u}_s$. Now use the formula given in the Appendix with

$$\Psi_1^{\text{new}} = \Psi_1 - \frac{\boldsymbol{v}_s\left(\boldsymbol{v}_s^T\Psi_1 + \boldsymbol{w}_s^T\Psi_2\right)}{\boldsymbol{v}_s^T\boldsymbol{v}_s} \tag{46}$$

$$\Psi_2^{\text{new}} = \Psi_2 - \frac{\boldsymbol{w}_s\left(\boldsymbol{v}_s^T\Psi_1 + \boldsymbol{w}_s^T\Psi_2\right)}{\boldsymbol{v}_s^T\boldsymbol{v}_s} \tag{47}$$

Plotting these new computations, it is possible to compare the original cost of targeting to the origin to the new cost obtained by targeting to the stable manifold minimizing $|\Delta V_1|$ and minimizing $|\Delta V_1|^2 + |\Delta V_2|^2$. As can be seen in Fig. 4, the second minimization

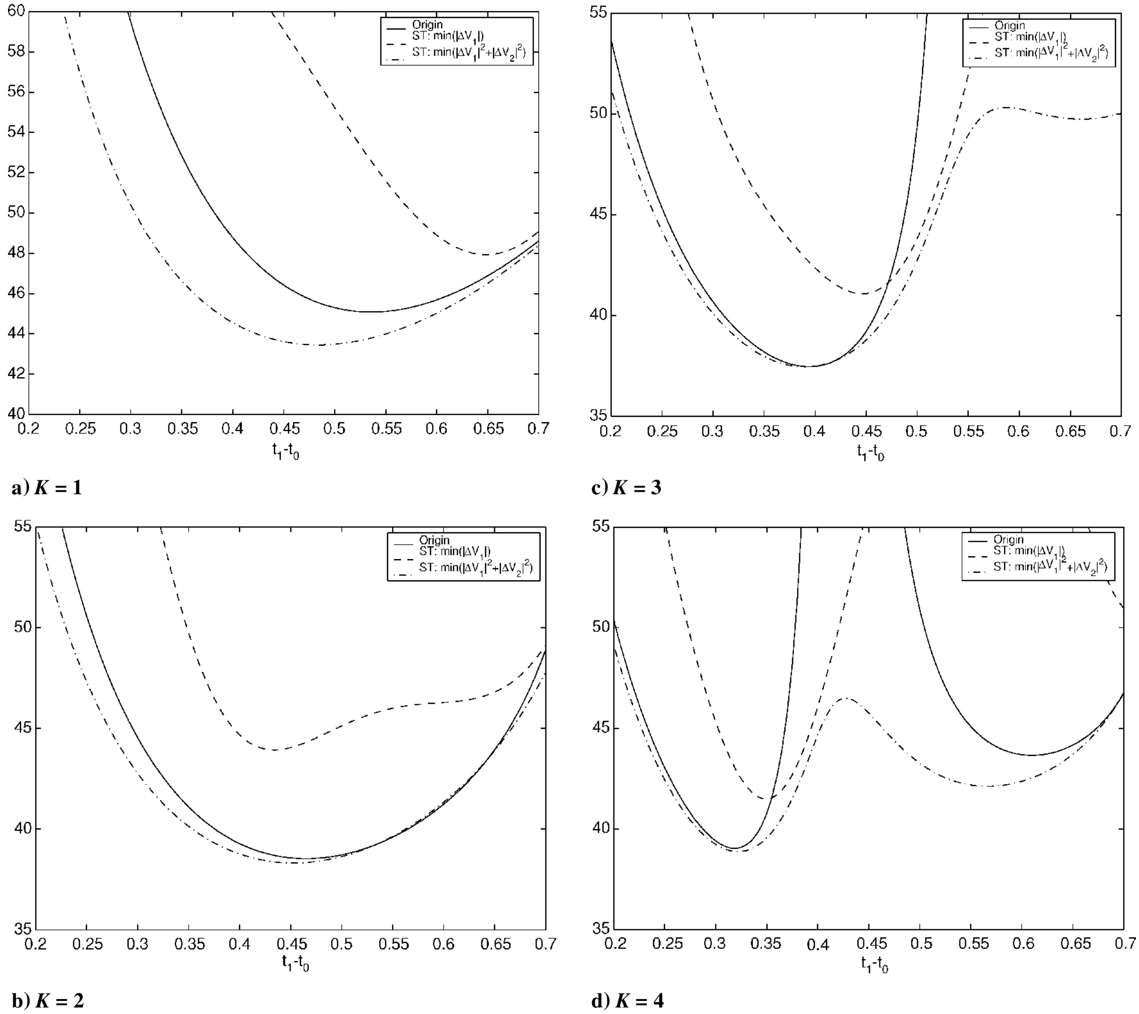

Fig. 4 Targeting the stable manifold: optimal cost.

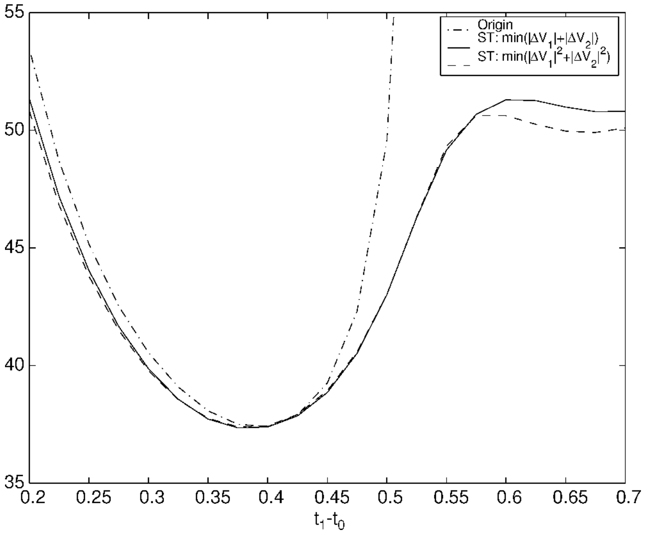

Fig. 5 Comparison for $k = 3$: $\min(|\Delta V_1| + |\Delta V_2|)$ and $\min(|\Delta V_1|^2 + |\Delta V_2|^2)$.

improves the results a little, whereas the first one gives worse results than targeting the origin. For $k = 1$, the results are significantly improved; however the minimal cost is still above the minimal cost obtained for $k = 3$. For $k = 3$, the new minimum is 37.45 instead of 37.46; it has only decreased marginally. Note also that for $k = 3$ the singularities (corresponding earlier to ϕ_{rv} being singular) have been removed by this method. As a result, the corrections can be performed at any time, which is an advantage.

Minimization of $|\Delta V_1| + |\Delta V_2|$

As already mentioned, finding the minimum of $|\Delta V_1| + |\Delta V_2|$ requires the solution of a polynomial of fourth order. To compare this solution with the preceding one, software was developed along the principle that, for a fixed interval $t_1 - t_0$ and fixed k such that $t_2 - t_1 = k(t_1 - t_0)$, n random errors are chosen following a Gaussian random distribution. Then for these random errors, the η coefficients, giving the position targeted on the stable manifold and minimizing $|\Delta V_1| + |\Delta V_2|$, are computed. The n random errors are considered as a sequence, meaning that they follow each other along the time axis. Figure 5 shows a comparison of the cost when the origin is targeted and the cost when the stable manifold is targeted, minimizing $|\Delta V_1| + |\Delta V_2|$ and minimizing $|\Delta V_1|^2 + |\Delta V_2|^2$. All of the curves are drawn for the same random sequences. The first point to note is that the results of using a sequence of 1000 maneuvers are close to the exact result given by the integration. Also note that minimizing $|\Delta V_1|^2 + |\Delta V_2|^2$ is almost identical to minimizing $|\Delta V_1| + |\Delta V_2|$.

Minimizing $|\Delta V_1 + \Delta V_2|$

Finally, we consider a strategy of minimizing $|\Delta V_1 + \Delta V_2|$ at each new step. As a consequence, at the time t_i, we want to find η_i that will minimize the norm $|\eta_i \boldsymbol{v}_s + \eta_{i-1}\boldsymbol{w}_s + \phi_1 \delta \boldsymbol{r}_i + \phi_2 \delta \boldsymbol{r}_{i-1}|$, where η_i must satisfy the sequence

$$\eta_i = -\frac{\boldsymbol{v}_s^T(\phi_1 \delta \boldsymbol{r}_i + \phi_2 \delta \boldsymbol{r}_{i-1})}{\boldsymbol{v}_s^T \boldsymbol{v}_s} - \frac{\boldsymbol{v}_s^T \boldsymbol{w}_s}{\boldsymbol{v}_s^T \boldsymbol{v}_s}\eta_{i-1} \tag{48}$$

If Eq. (48) is reinjected in the computation of $|\Delta V_1 + \Delta V_2|$, a cancellation occurs if v_s and w_s are parallel, which gives

$$|\Delta V_1 + \Delta V_2| = \left(Id - \frac{\boldsymbol{v}_s \boldsymbol{v}_s^T}{\boldsymbol{v}_s^T \boldsymbol{v}_s}\right)(\phi_1 \delta \boldsymbol{r}_i + \phi_2 \delta \boldsymbol{r}_{i-1}) \tag{49}$$

As a result, Eq. (41) can be used taking $\boldsymbol{v}_s = \phi_{rv}(t)^{-1}\boldsymbol{u}_s$. This computation is valid only when $\boldsymbol{v}_s$ is parallel to $\boldsymbol{w}_s$. Because $\boldsymbol{v}_s$ and $\boldsymbol{w}_s$ depend on $t_2 - t_1$, for each value of k, we need to change the possible values of $t_1 - t_0$ accordingly. Plotting $[\boldsymbol{v}_s(1)w_s(2) - w_s(1)v_s(2)]/(\boldsymbol{v}_s^T \boldsymbol{v}_s)$ vs $t_2 - t_1$ shows that these values of $t_2 - t_1$ exist; however, all of the corresponding values of the cost are above 40 and are still worse than targeting the origin.

For intervals of time $t_1 - t_0$ regularly distributed, simulations of the 1000 maneuvers show that the cost rapidly goes to infinity, which indicates that the spacecraft will diverge from the equilibrium point. Only for very small intervals of time around the time for which $\boldsymbol{u}_s$ is parallel to $\boldsymbol{v}_s$ will the spacecraft not diverge from its position. Focusing on these time intervals, we can find the values of the cost computed earlier.

Linear Quadratic Regulator Control Algorithm

Linear Quadratic Regulator Method

Now let us formulate the problem in terms of digital control, $\boldsymbol{x}(k+1) = G\boldsymbol{x}(k) + H\boldsymbol{u}(k) + \boldsymbol{w}(k)$, where

$$G = \Phi, \qquad H = \begin{bmatrix} 0 & 0 \\ 0 & 0 \\ 1 & 0 \\ 0 & 1 \end{bmatrix}, \qquad \boldsymbol{u}(k) = \Delta \boldsymbol{V}(k)$$

and $\boldsymbol{w}$ is a Gaussian noise representing the orbit determination error such that

$$E[\boldsymbol{w}(k)] = 0, \qquad E[\boldsymbol{w}(j)\boldsymbol{w}^T(k)] = \Lambda^{-1}\delta_{jk} = Q_w \delta_{jk}$$

With use of this equation, let us find the optimal control law $u(k)$ that will minimize

$$J = E\left[S_N + \sum_{k=0}^{N-1} \boldsymbol{x}^T(k)Q\boldsymbol{x}(k) + \boldsymbol{u}^T(k)R\boldsymbol{u}(k)\right] \tag{50}$$

with $S_N = \boldsymbol{x}^T(N)P(N)\boldsymbol{x}(N)$. Let

$$P(k) = Q + G^T P(k+1)G - G^T P(k+1)H \times [R + H^T P(k+1)H]^{-1} H^T P(k+1)G \tag{51}$$

$$K(k) = [R + H^T P(k+1)H]^{-1} H^T P(k+1)G \tag{52}$$

When these parameters are used, it can be shown[14] that the control vector that minimizes J is given by the equation $\boldsymbol{u}(k) = -K(k)\boldsymbol{x}(k)$. Finally,

$$J_{\min} = \boldsymbol{x}^T(0)P(0)\boldsymbol{x}(0) + E\left[\sum_{k=0}^{N-1} \mathrm{tr}[P(k+1)Q_w]\right] \tag{53}$$

Let us now consider the steady-state quadratic optimal control. Take the limit $N \to \infty$; the optimal control solution becomes a steady-state solution and the-time varying gain matrix $K(k)$ becomes a constant gain matrix K. For $N = \infty$, the performance index may be modified to

$$J = E\left[\sum_{k=0}^{\infty} \boldsymbol{x}^T(k)Q\boldsymbol{x}(k) + \boldsymbol{u}^T(k)R\boldsymbol{u}(k)\right] \tag{54}$$

Where the steady state matrix P is solution of the algebraic Riccati equation,

$$P = Q + G^T PG - G^T PH[R + H^T PH]^{-1} H^T PG$$

$$K = [R + H^T PH]^{-1} H^T PG$$

A problem arises with the cost function J because, as tr $[PQ_w]$ is finite and not necessarily equal to zero, J is infinite. However, as shown in the following, if

$$J = \lim_{k\to\infty} E[\boldsymbol{x}^T(k)Q\boldsymbol{x}(k) + \boldsymbol{u}^T(k)R\boldsymbol{u}(k)] \tag{55}$$

then $J = \mathrm{tr}\,[PQ_w]$. Taking $R = I$, we have

$$\overline{|\Delta V|^2} = \lim_{k\to\infty} \boldsymbol{u}^T(k)R\boldsymbol{u}(k) \tag{56}$$

$$J = \overline{|\Delta V|^2} + \lim_{k\to\infty} \overline{\boldsymbol{x}^T(k)Q\boldsymbol{x}(k)} \tag{57}$$

Let us now find $\overline{|\Delta V|^2}$. Let $P_X(k+1) = E[\boldsymbol{x}(k+1)\boldsymbol{x}^T(k+1)]$, then $P_X(k+1) = (G - HK)P_X(k)(G - HK)^T + Q_w$. Because the characteristic roots of $G - HK$ are inside the unit circle, the effects of the initial condition $P_X(0)$ gradually diminish, and P_X approaches a stationary value. This value is given by the solution of the Lyapunov equation

$$P_X = (G - HK)P_X(G - HK)^T + Q_w \tag{58}$$

Finally,

$$\lim_{k\to\infty} E[\boldsymbol{x}^T(k)Q\boldsymbol{x}(k)] = \mathrm{tr}[P_X Q] \tag{59}$$

$$\lim_{k\to\infty} E[\boldsymbol{u}^T(k)R\boldsymbol{u}(k)] = \mathrm{tr}\big[KP_XK^T\big] \tag{60}$$

and as a result,

$$\overline{|\Delta V|^2} = \mathrm{tr}[PQ_w] - \mathrm{tr}[P_X Q] = \mathrm{tr}\big[KP_XK^T\big] \tag{61}$$

The parameter studied in the preceding sections is $\overline{|\Delta V|}$. As a consequence, we need to estimate this parameter with the linear quadratic regulator (LQR) method to have a comparison between the two controls. First, $\sigma^2_{\Delta V} = \overline{|\Delta V|^2} - \overline{|\Delta V|}^2 \geq 0$ implies that $\overline{|\Delta V|} \leq \sqrt{(\mathrm{tr}[KP_XK^T])}$. Then, using

$$\boldsymbol{x}(k+1) = \sum_{j=0}^{k} (G - HK)^j \boldsymbol{w}(k-j) \tag{62}$$

we find

$$\Delta\boldsymbol{V}(k+1) = \sum_{j=0}^{k} \phi(j)\boldsymbol{w}(k-j) \tag{63}$$

with $\phi(j) = -K(G - HK)^j$. Still use the method of computation of $\overline{|\Delta V|}$ described in the Appendix, and this gives

$$\overline{|\Delta V(k)|} = \sqrt{2/\pi}\sqrt{\lambda + \mu}\quad \mathrm{elliptic}E\Big[\sqrt{2\mu/(\lambda+\mu)}\Big] \tag{64}$$

where λ and μ are finite series that converge rapidly to a solution that does not depend on k, which is consistent with the existence of a limit for $P_X(k)$.

When this method is used, it becomes necessary to check the average spacecraft distance from the origin. Indeed if the spacecraft drifts too far from the equilibrium point, the linearization approximation cannot be kept. The average distance from the origin can also be studied using the same method as earlier with a series for λ and μ. With $S = \mathrm{diag}(1, 1, 0, 0)$,

$$T = \begin{bmatrix} 1 & 0 & 0 & 0 \\ 0 & 1 & 0 & 0 \end{bmatrix}, \qquad \phi_d(j) = T(G - HK)^j$$

$$d(k+1) = \left|\sum_{j=0}^{k} \phi_d(j)\boldsymbol{w}(k-j)\right| \tag{65}$$

$$\lim_{k\to\infty} \overline{d(k)^2} = \mathrm{tr}[P_X S] \tag{66}$$

Implementation of LQR Method

Now the performance of the methods are compared (Fig. 6). For the average distance from the origin using the first method (d_p in Fig. 6), we compute the average distance in the case where $t_1 - t_0 = t_2 - t_1$. Three different matrices Q have been considered. $Q = 0.05S$ implies that there is nearly no requirement on the position of the spacecraft. As can be seen in Fig. 6b, the achievement in the cost is good, 30.6 instead of the previous 37.5, but the tradeoff is that the position is more than twice as far from the origin. $Q = 500$ implies that the requirement on the position is strong and, therefore, that the spacecraft will stay close to the origin. As expected, the best cost is now worse than 37.5 and equals 44.5. Considering the case $Q = 5S$, we find that the average distances from the origin are nearly the same for the two control methods. However, a new optimal cost is obtained of about 35.3. It seems that the LQR method improves the optimal cost without increasing the average distance of the spacecraft from the equilibrium point. Note that if we take the ratio $\sigma_r/\sigma_v = \omega/\sigma_{vd}$ with ω equal to the rotation rate of the moon around the Earth, we find that targeting the origin gives the optimal cost of 19.9 for $k = 3$, whereas the optimal costs for the LQR method are 16.5, 18, and 22.4 for $Q = 0.05S$, $Q = 5S$, and $Q = 500S$, respectively. Therefore, we can conclude that the LQR method gives better results than the method of targeting the equilibrium point in this case as well.

Comparison and Discussion of Optimal Approach

Testing the Validity of the Model

Our linear control has also been implemented using the nonlinear model. One must be careful in the implementation of the controller to take into account that the LQR method uses the previous state error to correct the trajectory, whereas the method that targets the origin uses the previous state error minus what the state would be if the model was behaving linearly.

The procedure of computation with the LQR method is as follows: From $\boldsymbol{x}(k)$, the nonlinear equations are integrated over the period T to obtain $\boldsymbol{x}(k+1)'$, where

$$\boldsymbol{x}(k+1) = \boldsymbol{x}(k+1)' - HK[\boldsymbol{x}(k) - \boldsymbol{x}_{\mathrm{eq}}] + \boldsymbol{w}(k)$$

The procedure of computation by targeting the equilibrium point $t_2 - t_1 = k(t_1 - t_0)$ is as follows:

1) From $x(k)$, the nonlinear equations are integrated over the period T to obtain $x(k+1)'$.

2) The case of the k first maneuvers, where only the correction ΔV_1 is performed, has to be considered separately. As a result, in this case $\boldsymbol{x}(n+1) = \boldsymbol{x}(n+1)' + \phi_1\boldsymbol{x}_{\mathrm{corr}}(n) + \boldsymbol{w}(n)$, whereas after kT, $\boldsymbol{x}(n+1) = \boldsymbol{x}(n+1)' + \phi_1\boldsymbol{x}_{\mathrm{corr}}(n) + \phi_2\boldsymbol{x}_{\mathrm{corr}}(n-k) + \boldsymbol{w}(n)$.

3) The computation of $\boldsymbol{x}_{\mathrm{corr}}(n)$ requires us to compute what the state would be if the model were behaving linearly, using $K_1 = -\phi_1$:

$$\boldsymbol{x}_{\mathrm{corr}}(n) = \boldsymbol{x}(k) - \boldsymbol{x}_{\mathrm{eq}} - \sum_{j=1}^{n} G^{n-j}(G - HK_1)\boldsymbol{x}_{\mathrm{corr}}(j-1)$$

for the k first steps, and

$$\boldsymbol{x}_{\mathrm{corr}}(n) = \boldsymbol{x}(k) - \boldsymbol{x}_{\mathrm{eq}} - \sum_{j=1}^{k} G^{k-j}(G - HK_1)\boldsymbol{x}_{\mathrm{corr}}(n+j-k-1)$$

for the following steps.

Once these models were implemented, we tested them to find what the maximum allowable variance is. For the LQR method, taking the values of variance computed before, we find that these values can be multiplied by 40,000. This means that the model can correct position errors of 40,000 km and velocity errors of 40 ms^{-1} in velocity, a rather large magnitude. For the method of targeting the equilibrium, the values can be multiplied by 32,000, 32,000, 24,000, and 900 for k = to 1, 2, 3, and 4, respectively. The lower value of 900 corresponds to the period $T = 0.4$ for $k = 4$. Indeed for this particular value, we have seen that the cost increases very rapidly because the matrix ϕ_{rv} is becoming singular.

Comparison Between Results of Simulations and Analytical Conclusions

To compare the results of the simulations and the results of the analytical conclusions, we took the scaling values of the Earth–sun system. Figures 7 and 8 give the accelerations necessary to control the spacecraft in the Earth–sun system in kilometers per second per year, Fig. 7 for the LQR method with $Q = 5S$ and Fig. (8) for the method of targeting the equilibrium with $k = 3$. Figures 7 and 8 have been generated with $N = 400$ maneuvers for the nonlinear model. As can be seen, the comparisons give good results, indicating that the nonlinear model will be close to the analytical computations

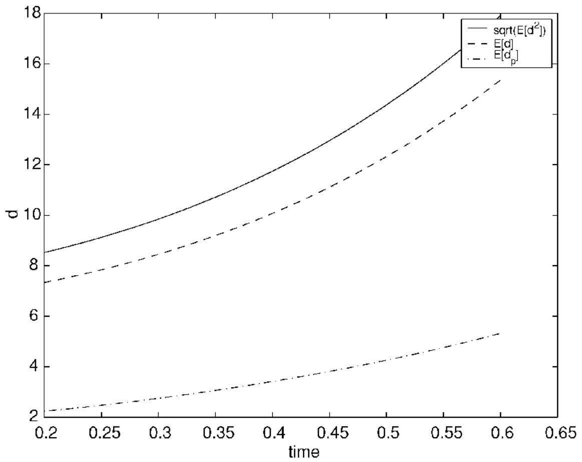

a) Average distance from the origin: Q = 0.05* diag(1, 1, 0, 0)

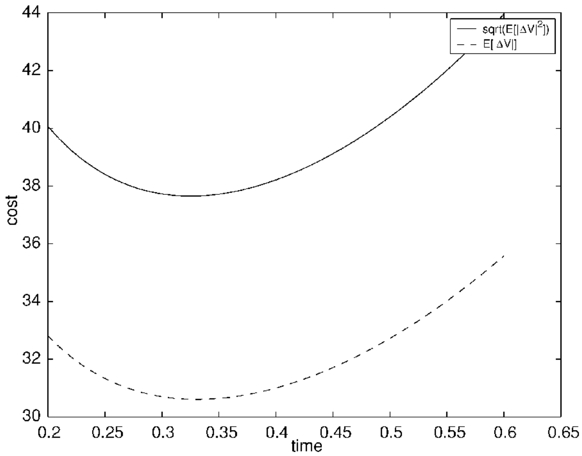

b) Cost of maneuvers Q = 0.05* diag(1, 1, 0, 0)

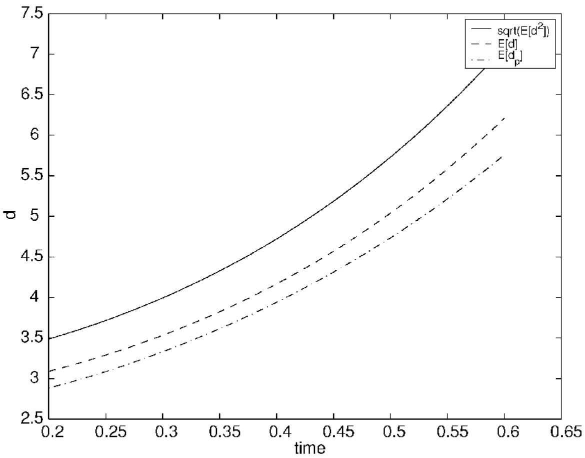

c) Average distance from the origin: Q = 5* diag(1, 1, 0, 0)

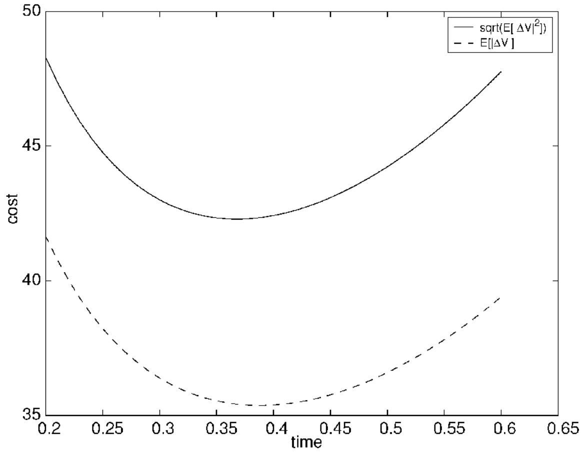

d) Cost of maneuvers Q = 5* diag(1, 1, 0, 0)

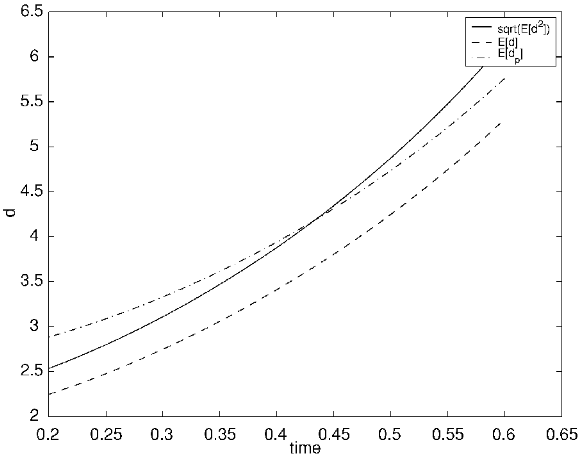

e) Average distance from the origin: Q = 500* diag(1, 1, 0, 0)

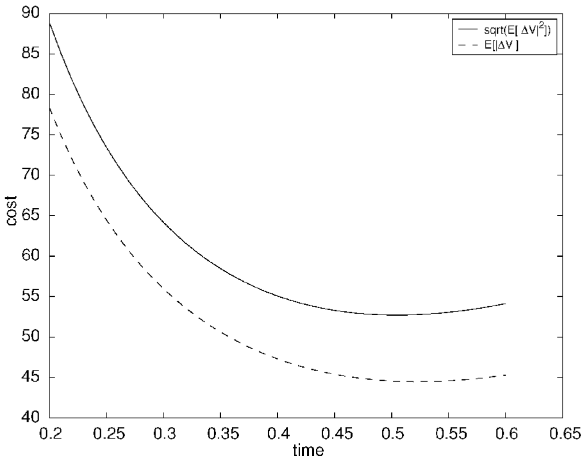

f) Cost of maneuvers Q = 500* diag(1, 1, 0, 0)

Fig. 6 LQR method: optimal cost.

made using the linear model. The nonlinear model seems to deviate more from the analytical solution for the LQR method, mainly due to the different scaling of the plots.

Application to the Restricted Three-Body Problem

Now let us write the nondimensional equations of the restricted three-body problem in two dimensions:

$$\ddot{x} - 2\dot{y} = x - \frac{(1-\mu)(x+\mu)}{[(x+\mu)^2 + y^2]^{\frac{3}{2}}} - \frac{\mu(x-1+\mu)}{[(x-1+\mu)^2 + y^2]^{\frac{3}{2}}} \tag{67}$$

$$\ddot{y} + 2\dot{x} = y - \frac{(1-\mu)y}{[(x+\mu)^2 + y^2]^{\frac{3}{2}}} - \frac{\mu y}{[(x-1+\mu)^2 + y^2]^{\frac{3}{2}}} \tag{68}$$

There are five equilibrium points for this system. Two of them, called L1 and L2, correspond to the two equilibrium points of the Hill problem, and μ corresponds to the mass ratio of the smallest body mass to the the sum of the two masses. For the Earth–sun system, μ is small, and the problem can be approximated by the Hill problem. However, for the Earth–moon system, $\mu = 0.0122$, and the Hill approximation gives quite different results from the restricted three-body problem, as will be shown.

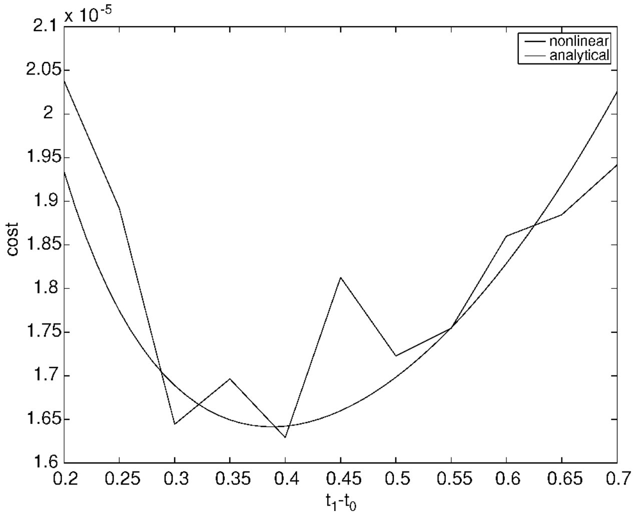

Fig. 7 LQR method: cost of nonlinear model vs cost of linear model.

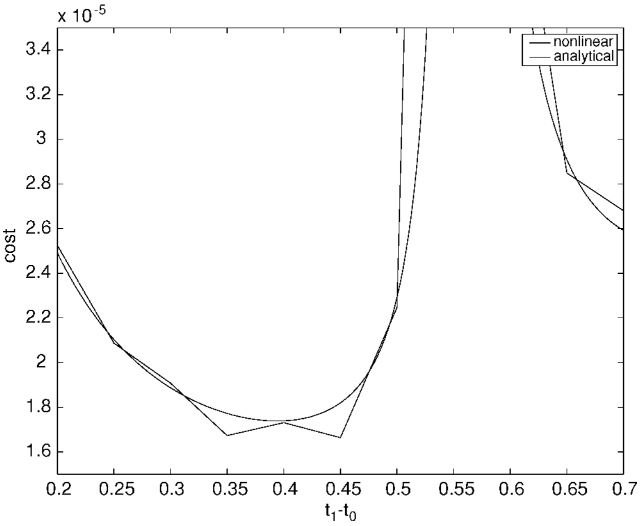

Fig. 8 Targeting the equilibrium: cost of nonlinear model vs cost of linear model.

The linearization around the equilibrium points $[x_{1,2}\ \ 0]$, where $x_1 = 0.99$, $x_2 = 1.01$ for the Earth–sun system and $x_1 = 0.837$, $x_2 = 1.156$ for the Earth–moon system, gives

$$\delta\dot{\boldsymbol{x}} = \begin{bmatrix} 0 & 0 & 1 & 0 \\ 0 & 0 & 0 & 1 \\ 1+2a & 0 & 0 & 2 \\ 0 & 1-a & -2 & 0 \end{bmatrix} \delta\boldsymbol{x} \tag{69}$$

with $a_i = (1-\mu)/|x_i+\mu|^3 + \mu/|x_i - 1 + \mu|^3$.

Solving the charateristic polynomial of this new matrix for these libration points gives two opposite real eigenvalues $\pm\lambda_1$ and two complex conjugate eigenvalues $\pm j\lambda_2$ as in the Hill problem. To compute $\Phi(t, t_0, \boldsymbol{x}_0)$, the polynomial decomposition of part one can still be used with the α_i [Eqs. (19–25)].

Let us compare the characteristic exponent λ_1 given by the two problems for the Earth–moon system. For $x_1 = 0.837$, $\lambda_1 = 2.93$, and for $x_2 = 1.156$, $\lambda_1 = 2.15$, whereas for the Hill problem, $\lambda_1 = 2.51$. When the results from the earlier part are used, these values imply that the optimal control period will be smaller for x_1 than the optimal period given by the Hill problem and greater for x_2. Tables 1 and 2 show a comparison of the results given by the restricted three-body problem with the results of the Hill problem. They show that the values predicted using the Hill problem are close to the values predicted by the restricted three-body problem for the Earth–sun system. For the Earth–moon system, the values predicted by the two models are quite different; however the results of the Hill problem are close to the average of the L1 and L2 results and, thus, can be used to estimate results. The errors made in the two methods are proportional, and the Hill problem gives an expected cost between 22 and 26% higher than the real cost for $x_2 = 1.156$ and gives an expected cost between 20 and 23% lower than the real cost for $x_1 = 0.837$. The optimal maneuver periods also change, as discussed earlier. Figures 9 and 10 show a comparison of these costs for the two systems and the two methods, with $x_1 = 0.99$ taken for the Earth–sun system and $x_1 = 0.837$ for the Earth–moon system. The results in the Earth–moon system are contracted in time because of the error made in the eigenvalues.

Table 1 LQR method: orbit determination uncertainties of $\sigma_{rd} = 10$ km, $\sigma_{vd} = 1 \times 10^{-5}$ km/s

Problem	S	Cost, km/s/period	Optimal spacing
		Earth–sun	
Hill	100	5.35×10^{-4}	28.5 days
	0.01	3.78×10^{-4}	18.6 days
Three-body	100	5.30×10^{-4}	28.5 days
$x_2 = 1.01$	0.01	3.74×10^{-4}	19.2 days
Three-body	100	5.39×10^{-4}	27.9 days
$x_1 = 0.99$	0.01	3.82×10^{-4}	18.6 days
		Earth–moon	
Hill	100	3.60×10^{-3}	45.42 h
	0.01	2.75×10^{-3}	33.03 h
Three-body	100	2.95×10^{-3}	52.6 h
$x_2 = 1.156$	0.01	2.17×10^{-3}	38.2 h
Three-body	100	4.89×10^{-3}	39.2 h
$x_1 = 0.837$	0.01	3.53×10^{-3}	27.9 h

Table 2 Targeting the equilibrium: orbit determination uncertainties of $\sigma_{rd} = 10$ km, $\sigma_{vd} = 1 \times 10^{-5}$ km/s

Problem	Cost, km/s/period	Optimal spacing
	Earth–sun	
Hill	4.70×10^{-4}	22.9 days
Three-body, $x_2 = 1.01$	4.65×10^{-4}	23.1 days
Three-body, $x_1 = 0.99$	4.75×10^{-4}	22.7 days
	Earth–moon	
Hill	3.36×10^{-3}	38.2 h
Three-body, $x_2 = 1.156$	2.66×10^{-3}	44.4 h
Three-body, $x_1 = 0.837$	4.32×10^{-3}	32.8 h

Application to Nonequilibrium Trajectories

The preceeding analyses have all been applied to the control of a spacecraft relative to an unstable equilibrium point. Although interesting and representative of the dynamics of a spacecraft in an unstable orbital environment, most space missions to libration points are flown in periodic or quasi-periodic orbits about the equilibrium points. The application of our analysis can be extended to this more difficult and realistic problem by using methods outlined by Scheeres et al.[8,10,15] In those papers, it was found that the analysis of orbit determination and control of an unstable halo orbit can be performed by approximating the state transition matrix between two times along the time-varying trajectory by the state transition matrix that satisfies the time-invariant equations of motion specified at a time within this interval.

Specifically, the motion of a spacecraft relative to its time-varying nominal orbit can be represented using the equations of motion linearized about the nominal trajectory

$$\delta\dot{\boldsymbol{x}} = A(t)\delta\boldsymbol{x} \tag{70}$$

where $A(t)$ is the time-varying partials matrix evaluated along the nominal trajectory. The solution to the time-varying system can be approximated over finite intervals of time as[8]

$$\Phi(t, t_0) = \exp[A(t_0)(t - t_0)] + \cdots \tag{71}$$

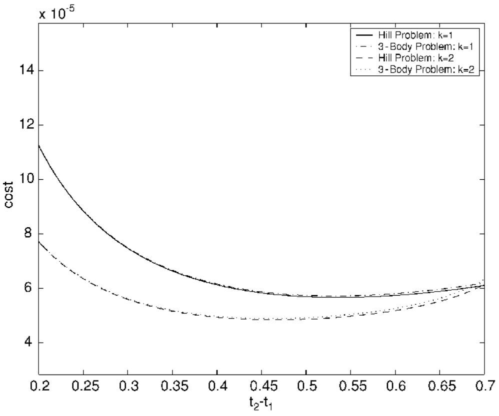

a) Earth–sun $k = 1, 2$

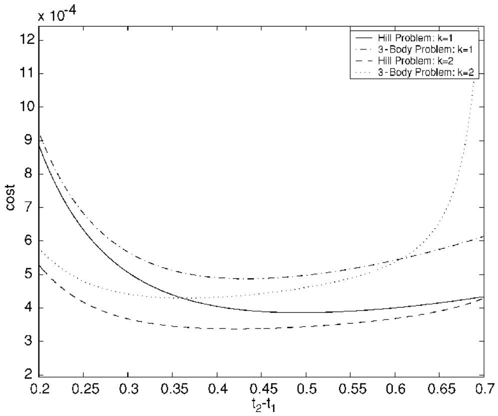

c) Earth–moon $k = 1, 2$

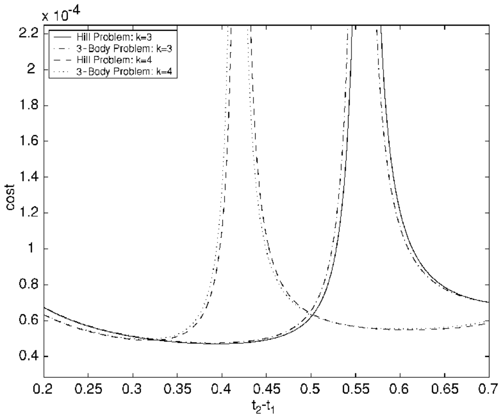

b) Earth–sun $k = 3, 4$

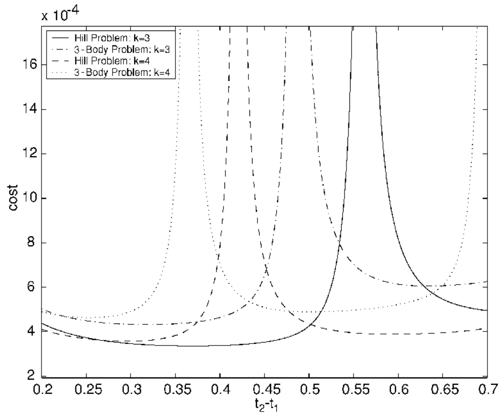

d) Earth–moon $k = 3, 4$

Fig. 9 Targeting the equilibrium: comparison of Hill problem and restricted three-body problem.

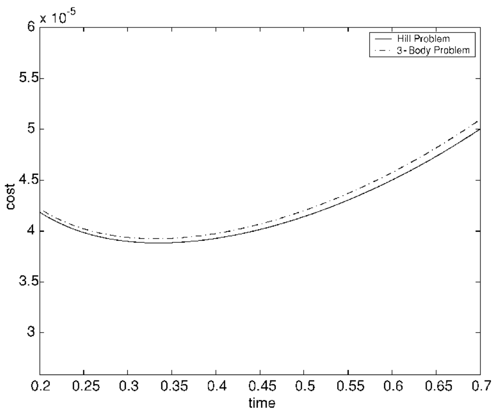

a) Earth–sun $Q = 0.1^{*}S$

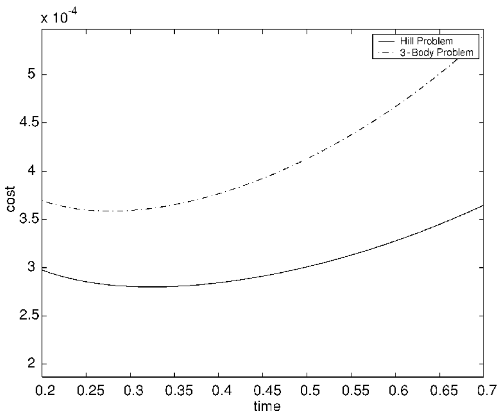

c) Earth–moon $Q = 0.1^{*}S$

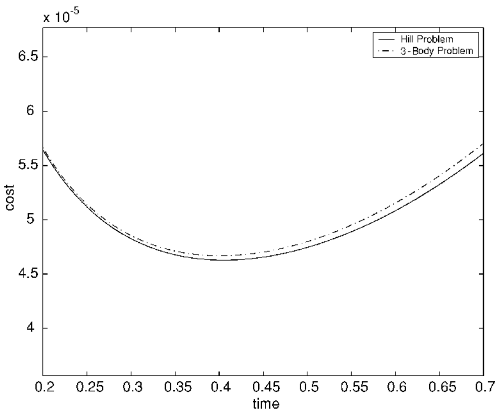

b) Earth–sun $Q = 0.1^{*}S$

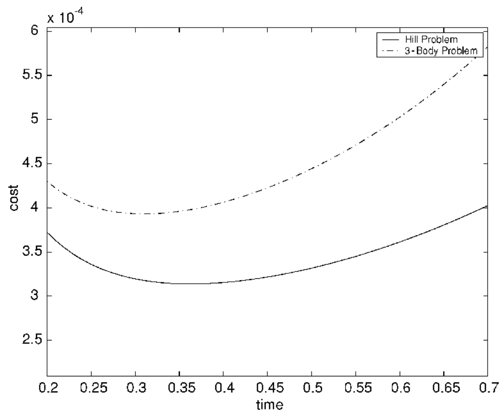

d) Earth–moon $Q = 0.1^{*}S$

Fig. 10 LQR method: comparison of Hill problem and restricted three-body problem.

where Φ satisfies Eq. (70) and the exponential term satisfies the time-invariant system found by keeping the time t_0 constant in $A(t_0)$. For the analysis of control and orbit determination phenomenon, which occur over time spans less than one orbit period, this approximation has been shown to be accurate.[15] Under this restriction, it is possible to carry out the same analyses as described in this paper. Thus, we expect to find a similar, optimal spacing for control maneuvers along unstable halo or quasi-periodic orbits in general.

For these applications, the optimal maneuver spacing would be computed from the local characteristic exponent of the linearized flow, defined as the unstable eigenvalue of the matrix $A(t)$. This implies that the optimal spacing of control maneuvers may vary along the orbit because the instantaneous characteristic exponents vary in time. However, we also note that these instantaneous characteristic exponents do not vary significantly within a periodic orbit. Thus, in analogy with the results for the equilibrium point, one could assume that the optimal spacing of control maneuvers along a periodic or quasi-periodic trajectory will be related to the Lyapunov characteristic exponent of the periodic or quasi-periodic orbit. A more detailed analysis of this will be considered in the future.

Conclusions

This paper compares different control strategies that can be implemented to control a spacecraft about an unstable equilibrium point. First, an optimal statistical cost has been found for simultaneous maneuvers targeting the equilibrium point. This first control approach has been extended to the more general method of targeting the stable manifold. We have shown that targeting the stable manifold does not improve the results. The LQR method and its tradeoff has been investigated, leading to improvements of the statistical cost. All of these results have been checked by nonlinear simulations. Finally, the optimal costs of the two controls have been compared for the Hill problem and the restricted three-body problem in the Earth–sun and moon–Earth systems. We have found that a maneuver spacing close to the characteristic time of the unstable eigenvalue is optimal in all cases.

Appendix: Procedure to Compute the Mean and Variance of $|\Delta V|$

The aim of this Appendix is to give a general method for the computation of the mean and variance of $|\Delta V|$. The mean is given by

$$\overline{|\Delta V|} = \int_{\infty} |\Delta V| f(\boldsymbol{x})\, \mathrm{d}\boldsymbol{x}$$

where f is the probability density function of a Gaussian distribution. The variance is given by

$$\sigma^2_{\Delta V} = \int_{\infty} |\Delta V|^2 f(\boldsymbol{x})\, \mathrm{d}\boldsymbol{x}$$

More explicitly, one can write

$$\overline{|\Delta V|} = \int_{\infty} |\Psi \boldsymbol{x}| \frac{\sqrt{|K|}}{(2\pi)^{N/2}} \exp\left(-\frac{1}{2}\boldsymbol{x}^T K \boldsymbol{x}\right) \mathrm{d}\boldsymbol{x} \tag{A1}$$

The main problem comes from the integration of the norm of $\Psi\boldsymbol{x}$. Let us write

$$\boldsymbol{u} = \begin{bmatrix} u_1 \\ u_2 \\ \vdots \\ u_N \end{bmatrix} = \begin{bmatrix} a_1^T \\ a_2^T \\ \vdots \\ a_N^T \end{bmatrix} \boldsymbol{x} = A\boldsymbol{x} \tag{A2}$$

where

$$\begin{bmatrix} a_1^T \\ a_2^T \end{bmatrix} = \Psi$$

and A is a $N \times N$ matrix. Let us assume rank $(\Psi) = 2$ so that A can be chosen to be nonsingular. With $\boldsymbol{u}$ as the new variable, introduce $H = A^{-T} K A^{-1}$, with $\mathrm{d}\boldsymbol{x} = \mathrm{d}\boldsymbol{u}/|A| = (|H|/|K|)^{1/2}\, \mathrm{d}\boldsymbol{u}$, where $|.|$ stands for the determinant of a matrix. It is possible to write the new expression of the integral

$$\overline{|\Delta V|} = \int_{\infty} \sqrt{u_1^2 + u_2^2} \frac{\sqrt{|H|}}{(2\pi)^{N/2}} \exp\left(-\frac{1}{2}\boldsymbol{u}^T H \boldsymbol{u}\right) \mathrm{d}\boldsymbol{u} \tag{A3}$$

Then if H is a diagonal matrix of the form $H = \mathrm{diag}(\alpha \;\; \beta \;\; 1 \;\; 1)$, integrating over $u_3, \ldots, u_N$, the integral takes the new form

$$\overline{|\Delta V|} = \frac{1}{2\pi} \int_{\infty} \sqrt{u_1^2 + u_2^2} \exp\left(-\frac{\alpha u_1^2 + \beta u_2^2}{2}\right) \sqrt{\alpha\beta}\, \mathrm{d}u_1\, \mathrm{d}u_2 \tag{A4}$$

Let us now examine the hypothesis of $H = \mathrm{diag}(\alpha \;\; \beta \;\; 1 \;\; 1)$ more closely, $A^T H A = K$ is equivalent to

$$\alpha a_1 a_1^T + \beta a_2 a_2^T + a_3 a_3^T + \cdots + a_N a_N^T = K \tag{A5}$$

Therefore, taking the orthogonal x to $(a_2, \ldots, a_N)$ gives $\alpha a_1 a_1^T x = Kx \Leftrightarrow \alpha(a_1^T x) a_1 = Kx$. As a result, $x = K^{-1} a_1$ must be orthogonal to a_2. This is only true for a particular matrix K. Because the integration must be performed for every K, a choice other than a_2 is needed in A. Let us introduce the new notation:

$$\Psi = \begin{bmatrix} a_1 \\ \overline{a_2} \end{bmatrix} \tag{A6}$$

$$\gamma = \frac{a_1^T K^{-1} \overline{a_2}}{a_1^T K^{-1} a_1} \tag{A7}$$

The last equality is possible for every $a_1 \neq 0$ because our information matrix and its inverse are positive definite. Let

$$a_2 = \overline{a_2} - \gamma a_1 \tag{A8}$$

Then $a_2^T K^{-1} a_1 = 0$. Finally, as we assumed rank$(\Psi) = 2$, a_1 and a_2 are independent.

Now let us prove that if a_k, $k \leq N$, is orthogonal to $(K^{-1}a_1, \ldots, K^{-1}a_{k-1})$, then a_k is independent of $(a_1, \ldots, a_{k-1})$. Let $\lambda_1, \ldots, \lambda_{k-1}$ not all equal to 0 such that

$$a_k = \sum_{j=1}^{k-1} \lambda_j a_j$$

Then for all $i \in [1, k-1]$: $\lambda_i a_i^T K^{-1} a_i = 0$. Because K^{-1} is positive definite, it gives $\lambda_i = 0$, a contradiction.

Finally when a_3 is taken in the orthogonal of $(K^{-1}a_1, K^{-1}\overline{a_2})$, a_3 is normalized such that $a_3^T K^{-1} a_3 = 1, \ldots, a_N$ in the orthogonal of $(K^{-1}a_1, \ldots, K^{-1}a_{N-1})$, a_N is normalized such that $a_N^T K^{-1} a_N = 1$, $(a_1, \ldots, a_N)$ is a basis. As a result, A is nonsingular, and

$$AK^{-1}A^T = H^{-1} \Leftrightarrow H = A^{-T} K A^{-1} \tag{A9}$$

Here α and β are given by

$$\alpha^{-1} = a_1^T K^{-1} a_1 \tag{A10}$$

$$\beta^{-1} = a_2^T K^{-1} a_2 = \overline{a_2}^T K^{-1} \overline{a_2} - \frac{\left(a_1^T K^{-1} \overline{a_2}\right)^2}{\left(a_1^T K^{-1} a_1\right)} \tag{A11}$$

These definitions give $|\Psi x| = [(a_1^T x)^2 + (a_2^T x + \gamma a_1^T x)^2]^{1/2}$. Now $|\Phi \boldsymbol{x}_0| = \sqrt{(1+\gamma^2)u_1^2 + u_2^2 + 2\gamma u_1 u_2}$ with $u_1 = a_1^T x$, $u_2 = a_2^T x$. Thus, as a consequence,

$$\overline{|\Delta V|} = |\Phi \boldsymbol{x}_0| \exp\left[-\left(\alpha u_1^2 + \beta u_2^2\right)/2\right] \sqrt{\alpha\beta}\, \mathrm{d}u_1\, \mathrm{d}u_2 \tag{A12}$$

Taking for the new variables $(v_1, v_2) = (\sqrt{\alpha}u_1, \sqrt{\beta}u_2)$ and then changing to polar coordinates gives the following new expression for the integral:

$$\overline{|\Delta V|} = \frac{1}{2\pi}\int_{\infty} C_\theta \rho^2 \exp[-(\rho^2/2)]\,\mathrm{d}\rho\,\mathrm{d}\theta \tag{A13}$$

with

$$C_\theta = \sqrt{\frac{(1+\gamma^2)\cos\theta^2}{\alpha} + \frac{\sin\theta^2}{\beta} + \frac{2\gamma\cos\theta\sin\theta}{\sqrt{\alpha\beta}}} \tag{A14}$$

To compute the integral of C_θ, let us write

$$C_\theta = \sqrt{\lambda + 0.5[(1+\gamma^2)/\alpha - 1/\beta]\cos 2\theta + \left(\gamma\big/\sqrt{\alpha\beta}\right)\sin 2\theta} \tag{A15}$$

with

$$\lambda = 0.5[(1+\gamma^2)/\alpha + 1/\beta]$$

Then, when $\mu \neq 0$ is assumed, $\overline{|\Delta V|}$ is given by

$$\overline{|\Delta V|} = \frac{1}{\sqrt{2\pi}}\int_0^{\pi} \sqrt{\lambda + \mu\cos(2\theta)}\,\mathrm{d}\theta \tag{A16}$$

with

$$\lambda = \left(a_1^T K^{-1} a_1 + \overline{a_2}^T K^{-1}\overline{a_2}\right)\big/2 \tag{A17}$$

$$\mu = \sqrt{\left(a_1^T K^{-1} a_1 - \overline{a_2}^T G^{-1}\overline{a_2}\right)^2\big/4 + \left(a_1^T K^{-1}\overline{a_2}\right)^2} \tag{A18}$$

More explicitly,

$$\overline{\Delta V} = \sqrt{2/\pi}\sqrt{\lambda+\mu}\quad \text{elliptic}E\left[\sqrt{2\mu/(\lambda+\mu)}\right] \tag{A19}$$

where elliptic$E$ is defined as

$$\text{elliptic}E(k) = \int_0^{\pi/2} (1 - k^2\sin^2\theta)^{\frac{1}{2}}\,\mathrm{d}\theta \tag{A20}$$

and is the complete elliptic integral of the second kind.

It is easy to check that the integration is still valid when $\mu = 0$. The other particular case is when $\mathrm{rank}(\Psi) = 1$. In this case, it is trivial to check that $\overline{|\Delta V|} = \sqrt{2/\pi}\sqrt{\lambda}$. For this matrix Ψ, because $\lambda = \mu$ and elliptic$E$ $(1) = 1$, the preceding formula gives the same result.

The variance of the statistical cost of these maneuvers is fairly easy to compute once this method has been developed for the mean,

$$\sigma_{\Delta V}^2 = \int_{\infty} |\Delta V|^2 f(\boldsymbol{x}_0)\,\mathrm{d}\boldsymbol{x}_0 - \overline{|\Delta V|}^2 \tag{A21}$$

$$\sigma_{\Delta V}^2 = \frac{1}{2\pi}\int_{\infty} C_\theta^2\rho^3\exp\left(-\frac{\rho^2}{2}\right)\mathrm{d}\rho\,\mathrm{d}\theta - \overline{|\Delta V|}^2 \tag{A22}$$

$$\sigma_{\Delta V}^2 = 2\lambda - \frac{2}{\pi}(\lambda+\mu)\quad \text{elliptic}E^2\left(\sqrt{\frac{2\mu}{\lambda+\mu}}\right) \tag{A23}$$

Acknowledgment

The work described here was funded in part by the Interplanetary Network Technology Program by a grant from the Jet Propulsion Laboratory, California Institute of Technology, which is under contract with NASA.

References

[1] Battin, R. H., *An Introduction to the Mathematics and Methods of Astrodynamics*, AIAA Education Series, AIAA, New York, 1987, pp. 543–549.

[2] Farquhar, R., Muhonen, D. P., Newman, C. R., and Heuberger, H. S., "Trajectories and Orbital Maneuvers for the First Libration-Point Satellite," *Journal of Guidance and Control*, Vol. 3, No. 6, 1980, pp. 549–554; also AIAA Paper 80-4123, 1980.

[3] Howell, K. C., and Pernicka, H. J., "Stationkeeping Method for Libration Point Trajectories," *Journal of Guidance, Control, and Dynamics*, Vol. 16, No. 1, 1993, pp. 151–159.

[4] Howell, K. C., and Gordon, S. C., "Orbit Determination Error Analysis and a Station-Keeping Strategy for Sun-Earth L_1 Libration Point Orbits," *Journal of the Astronautical Sciences*, Vol. 42, No. 2, 1994, pp. 207–228.

[5] Jones, B. L., and Bishop, R. H., "Rendezvous Targeting and Navigation for a Translunar Halo Orbit," *Journal of Guidance, Control, and Dynamics*, Vol. 17, No. 5, 1994, pp. 1109–1114.

[6] Cielaszyk, D., and Wie, B., "New Approach to Halo Orbit Determination and Control," *Journal of Guidance, Control, and Dynamics*, Vol. 19, No. 2, 1996, pp. 266–273.

[7] Gomez, G., Llibre, J., Martinez, R., and Simo, C.,"Dynamics and Mission Design Near Libration Points," *World Scientific Monograph Series in Mathematics*, Vol. 2, World Scientific, Singapore, Republic of Singapore, 2001, pp. 7–57.

[8] Scheeres, D. J., Hsiao, F.-Y., and Vinh, N. X., "Stabilizing Motion Relative to an Unstable Orbit: Applications to Spacecraft Formation Flight," *Journal of Guidance, Control, and Dynamics*, Vol. 26, No. 1, 2003, pp. 62–73.

[9] Dunham, D. W., and Roberts, C. E., "Stationkeeping Techniques for Libration-Point Satellites," *Journal of the Astronautical Sciences*, Vol. 49, No. 1, 2001, pp. 127–144.

[10] Scheeres, D. J., Han, D., and Hou, Y., "Influence of Unstable Manifolds on Orbit Uncertainty," *Journal of Guidance, Control, and Dynamics*, Vol. 24, No. 3, 2001, pp. 573–585.

[11] Wilson, R. S., Howell, K. C., and Lo, M. W., "Optimization of Insertion Cost for Transfer Trajectories to Libration Point Orbits," American Astronautical Society, Paper AAS 99-401, Aug. 1999.

[12] Serban, R., Koon, W. S., Lo, M. W., Marsden, J. E., Petzold, L. R., Ross, S. D., and Wilson, R. S., "Halo Orbit Mission Correction Maneuvers Using Optimal Control," *Automatica*, Vol. 38, 2002, pp. 571–583.

[13] Brouwer, D., and Clemence, G. M., *Methods of Celestial Mechanics*, Academic Press, New York, 1961, pp. 335–339.

[14] Ogata, K., *Discrete-Time Control Systems*, Prentice–Hall, Englewood Cliffs, NJ, 1987, pp. 912–914.

[15] Hsiao, F.-Y., and Scheeres, D. J., "The Dynamics of Formation Flight About a Stable Trajectory," American Astronautical Society, Paper AAS 02-189, Feb. 2002.